ANALYSIS OF LEVEL SET BASED NOVEL GENERIC MODEL FOR CROSSHATCHED TEXTURE SEGMENTATION

Prabhakar K.[1*], Sadyojatha K.M.[2]

Abstract

Visual textures are important for numerous scientific research domains like drug discovery, medical imaging, nano-scale chemical imaging studies, and molecular modeling. Texture studies in identifying drug shelf life and vegetable fungal studies are also upcoming domains of research to maintain the highest quality of products. Over the decades, the surface texture, carbon capturing, and chemical compounds like enamel coating in various industrial applications have been evaluated to improve visual analysis methods. Hence, the proposed study focused on the improvement of visual texture analysis. In image processing tasks, texture is the crucial component of using humane visual models for differentiating different targets in a necessary scenario. This study uses a variational model founded on the standard set for cross-hatched texture segmentation. The proposed model's functionality is endorsed on the Brodatz texture dataset in this research. The cross-hatched texture segmentation in the reduced image resolution texture is challenging because of the computational and storage requisites. The previously mentioned issues have been treated by applying a variational model according to the standard set that allows successful segmentation in low- and high-resolution graphics with an assortment of the filter size. In the proposed model, the multi-resolution characteristic acquired from the frequency domain filters improves the significant difference among the areas of cross-hatched textures with low-intensity disparities. Then, the resulting graphics are bundled by way of a level set-based active contour model that tackles the segmentation of cross-hatched texture imagery. The noise introduced during the segmentation procedure is eradicated by morphological refinement. The trials carried out on the Brodatz texture dataset exhibited the performance of the proposed model and the outcomes attained are authenticated regarding Intersection over the Union (IoU) index, accuracy, precision, f1-score, and recall. The intensive, unique analysis reveals that the proposed model systematically segments the region of interest in close correspondence with the main image. The proposed segmentation model with a multi-support vector machine has accomplished a classification accuracy of 99.82%, which is remarkable compared to the comparative model, like a modified convolutional neural network with a whale optimization algorithm. The proposed model nearly confirmed 0.11% betterment in classification accuracy appropriate to the existing model. Hence, the proposed study can be used for texture analysis as a generic solution for medical, drug/molecular chemical manufacturing, industrial, and agricultural domains.

Keywords: crosshatched texture, level set, morphological processing, multi-resolution, texture segmentation

[1*]Ballari Institute of Technology and Management, Department of Electronics and Communication Engineering, Ballari, India
[2]Ballari Institute of Technology and Management, Department of Electronics and Communication Engineering, Ballari, India

***Corresponding Author:** Prabhakar K.
*Ballari Institute of Technology and Management, Department of Electronics and Communication Engineering, Ballari, India

DOI: 10.53555/ecb/2022.11.11.95

1. Introduction

Nowadays, graphic evaluation is becoming among the distinguished methodologies for visual texture evaluation. In the agro-chemical domain, the detection of biopesticide layer on fruits and vegetables, the detection of ripped fruit levels, etc, are being examined for enhanced precision. Computer vision-based systems have currently been utilized in huge food and agricultural-based sectors to select different fruits and vegetables [1] as agriculture has become more than merely an approach to feed ever-growing masses. It is crucial regardless of where. In addition, more than seventy percent of the human population of an Asian country relies upon farming which in turn suggests that it feeds a good array of individuals. The primary need is to reflect on reduced crop quality mainly because of disease. Finding disease may be crucial to prevent agricultural losses [2].

In other scenarios, corrosion can be described as a chemical progression triggered by chemical and electrochemical tendencies. Certainly, there are distinct types of corrosion, such as general corrosion, that happens as evenly distributed nonprotective flakes of rust and pitting, a localized point of corrosive attack. Corrosion produces about the metal pipe surface, leading to decreased pipe service life and increased building maintenance cost [3]. Corrosion analysis can be carried out by applying visual texture analysis to stop the hazards of pipe leakages.

In the pharmaceutical industry, drug development is extremely costly and time-consuming. Commonly, US $1-1.5 billion and many years are believed to be required to advance a new drug before considerable clinical analysis. As a visual computational analysis approach, micro-CT imaging can reform the quality of current drug discovery methods. Researchers constantly strive to make micro-CT imaging more beneficial for quantification and visualization of a new drug outcome in a speedy and noninvasive way [4]. Even though the application of plasmonic structures in medicine has been growing swiftly, vital advancements in using plasmonics AuNPs have yet to be well described and outlined. Subsequently, it is essential to research optical entangling principles for optical cooling, imaging, binding, sorting such as tweezers, and shipping for drug delivery using optical energies [5]. Such discoveries can further be used to analyze chemical compound studies. Pill classification and identification are critical tasks in controlling the wrong use of medication. Certainly, there is a growing demand for automation for these kinds of tasks due to its inherent difficulty. The Food and Drug Administration (FDA) determines the different visual appearance of pills based on their shape, color, texture, and imprint information. [6].

Image de-noising is the disposal of noise from a noisy graphic to reestablish the authentic image. On the other hand, seeing that noise, edge, and texture are high-frequency elements, it is challenging to differentiate them in de-noising, so the de-noised images may predictably lose several details. In general, recovering significant information from noisy images in noise extraction to get high-quality graphics is essential today. [7]. There is a distinct pattern for enhancing efficiency and functionality in the industrial sector by combining new cutting-edge ICT solutions that are reshaping the industrial development paradigms, as in the Industry 4.0 initiative. Optical resolution photoacoustic microscopy (OR-PAM) is extensively employed in biology, medicine, and nanotechnology research. Using the collaboration of sharp-focused pulsed laser and high-sensitivity detection of fast thermal expansion-induced ultrasonic signals, OR-PAM offers both an optical-diffraction limited lateral resolution of micrometers and an imaging depth of millimeters [8]. Visual Computing solutions can play a key role in this strengthening procedure, consequently becoming essential in recognizing the Operator 4.0 vision [9].

Besides this, visual texture analysis is significant for using augmented reality (AR) as an element of entertainment and gaming in multi-player gaming, computer games, broadcasting, and multimedia videos. AR in medicine consists of using AR in medical treatment, training, surgery, and post-medical remedies. AR in retail was outlined relating to its applications in advertising campaigns, promotion, fashion retail, and online shopping [10]. Image texture is among the most significant elements of many images, incorporating medical images. Visualization using numerous medical imaging strategies symbolizes the properties of interior organs and tissues in terms of texture. The texture of the cross-sections of such structures, discovered by tomographic imaging, gives details that a classification process can further reinforce. [11].

Gradient-based texture investigation methods have become preferred in computer vision and image processing and have many applications incorporating medical image analysis. [12]. Classifying texture is a distinguished stage in pattern recognition complications. Hand Crafted Texture features or Texture descriptors effectively determine and classify diverse textures. Deep learning-based approaches can also classify and determine texture images [13]. Another sector for texture analysis is soil analysis in construction

agricultural functions. The physical and chemical properties of the soil usually play an essential role in precision and smart farming. Soil images are enhanced with diverse stages like pre-processing soil images for image enhancement, extracting the region of interest for segmentation, and analyzing the texture for the feature vector [14].

Texture classification has drawn much interest as an important step in pattern recognition and image processing. It is preferred in many applications, such as medical imaging, remote sensing, signature verification, script recognition, and face analysis. A powerful texture feature needs to have a positive tradeoff between high computational efficiency and unique information rendering [15]. On the other hand, Convolutional Neural Networks (CNN) have become a well-researched tool for various computer vision applications [15]. One of the main components of its success is the principle of transfer learning (TL), which is a class of approaches that allow pre-trained CNN models to achieve good results in domains with little labeled data [16].

Texture segmentation is partitioning an image into regions by distinctive textures containing similar groups of pixels. Cross-hatched texture in geological functions is significant and is the necessary surface characteristic in the cylinder bore produced from the focusing process [17]. Also, cross-hatched texture analysis is beneficial for analyzing variation land-cover features, which consist of natural and artificial objects, leading to the advent of spectrally identical features. Objects in urban areas tend to have similar spectral responses that can conveniently be misclassified from one to another, for example, in the case of trees and grass and asphalt building roofs and roads [18]. Landslide inventory mapping studies have received special attention from many specialists. In compliance with this circumstance, the existing study developed a semi-automatic GIS-based inventory mapping for locating landslides using a multi-resolution segmentation process, the first phase of Object-Oriented Analyses (OOA) [19].

As visual texture analysis is significant to numerous application domains, this study aims to segment the cross- hatched textures and to select the filter size in order to enhance the dissimilarity between regions with low-intensity variations. Hence, the filter size must be selected cautiously, because when the filter size is large, it causes uncertainties across the boundary regions and if small, then perhaps, it fails to confine certain variations in a few textures. The accurate descriptor and exact filter size are the necessary attributes for good texture segmentation. The main contributions are listed as follows:

- Used histogram equalization technique that improves the contrast of the collected images, which are acquired from the Brodatz texture dataset.
- Developed a precise model for the selection of the filter size. Further, the texture segmentation for crosshatched texture images is done in an unsupervised way. Analysis of Level Set based Novel Generic Model for Crosshatched Texture Segmentation is proposed for texture segmentation.
- The experimental results are validated by using different evaluation measures known as the IoU index, precision, f1-score, recall and accuracy. The segmentation results of the proposed model are compared with the Mix-Normalized-Cut (MixNCut) model, and the classification results are compared with the modified Convolutional Neural Network (CNN) with Whale Optimization Algorithm (WOA). The proposed segmentation model obtains near-perfect accuracy on all crosshatched texture images acquired from Brodatz texture dataset. The proposed model effectively sorts image data into interpretable information and it is utilized in an extensive range of applications like remote sensing, and medical imaging, Industrial application, image retrieval, etc.

This research article is organized as follows: research papers related to texture image segmentation and classification are surveyed in Section 2. The mathematical and theoretical explanation of the proposed model is specified in Section 3. The experimental outcome of the proposed model is stated in Section 4, and the conclusion of this work is mentioned in Section 5.

2. Literature Study

Based on the proposed research, this study presents the existing methods developed during various existing research.

The Prague texture segmentation data-generator and benchmark is a web-based service designed to mutually compare and rank different static and dynamic texture and image segmenters to find optimal parametrization of a segmenter and support the development of new segmentation and classification methods. The benchmark verifies segmenter performance characteristics on potentially unlimited monospectral, multispectral, satellite, and bidirectional texture function (BTF) data using an extensive set of over forty prevalent criteria [20]. The author suggested a deep learning-based image segmentation method to

segment the key areas in mineral images using morphological transformation to process mineral image masks. This investigation explores aspects of the deep learning-based mineral image segmentation model, including backbone selection, module configuration, loss function construction, and its application in mineral image classification [21].

In another research, the author recommended a segmentation method by designing an enhanced fuzzy-based K-means clustering algorithm, further compared with K-means and fuzzy C-means clustering methods. The geometric, texture, and color-based features are used in the feature extraction [22].

As a medical imaging texture researcher, the author developed automatic and semi-automatic image-based approaches for breast cancer diagnosis. In order to prevent, diagnose, and treatment of breast cancer, different imaging modalities have been developed. Computer-based imaging technologies are important in helping pathologists make decisions [23].

The early prediction of neoadjuvant chemotherapy outcomes is important in facilitating a personalized paradigm for breast cancer therapeutics. The author investigated quantitative computed tomography parametric imaging in conjunction with machine learning techniques to predict locally advanced breast cancer tumor response to neoadjuvant chemotherapy. Textural and second derivative textural features of CT images of patients diagnosed were analyzed before the initiation of neoadjuvant chemotherapy to quantify intra-tumor heterogeneity [24]. Image segmentation, texture analysis, principle component analysis (PCA), and support vector machine (SVM) were applied as previously described. First, a segmentation algorithm was used, which extracts relevant sub-images from each B-scan. Figure 1 illustrates the processing steps from the original B-scan to the segmented image, including median filtering to enable smooth edge detection, followed by Canny edge detection and thresholding using Otsu's method to determine the region of interest (ROI) [25].

Artificial intelligence (AI)–based solutions have the potential to help diagnose the COVID-19 pandemic effectively. In another study, the author reproduced convolutional neural network (CNN) models such as ResNeXt, Channel Boosted CNN, DenseNet, AlexNet, and VGG 16 to identify the presence of COVID-19 before they reach mass scale. Gaussian distribution theory was used to build a model for the transmission of coronavirus [26]. The author presented the novel application of Deep Support Vector Machine (DSVM), a fusion of DL and SVM to PolSAR image classification. Two PolSAR images of the Flevoland region in the Netherlands and Winnipeg in Canada are used as test beds for the experiment. The Lee filter filters the images to suppress the speckle noise in the images. The DSVM classifier is implemented with four kernel functions: Exponential Radial Basis Function (ERBF), Gaussian Radial Basis Function (GRBF), neural, and polynomial [27].

The author developed a multiclass support vector machines (MSVMs) based fault classification approach for fault diagnosis of ball bearings. The one-dimensional vibration signals are converted to two-dimensional grayscale images, resulting in textural patterns, which are then enhanced using the wave atom transform. Features such as semivariance, skewness, and entropy are extracted from the texture images, and the MSVM is then trained using feature matrices generated from feature vectors [28]. The author developed a dental caries-level classification system based on image processing and machine learning methods. The author conducted the first step to analyze and discover the extraction results from the Gray Level Co-Occurrence Matrix algorithm. After successfully extracting the features, the author completed the classification using a Support Vector Machine (SVM) and K-nearest neighbors (KNN). Both machine learning methods are analyzed and used to obtain better alternatives to the classification results [29].

3. Methodology

In recent decades, the possibility of inaccurate segmentation has been high when the parameters are selected voluntarily at the feature extraction or segmentation stage. Additionally, the supervised texture segmentation schemes require a priori knowledge, and it may not be viable to provide information regarding the number of texture regions and the type of textures to be segmented if the image volume is as large as a set of images in art galleries, large numbers of satellite imagery, etc. The supervised texture segmentation techniques make it difficult to manually provide prior knowledge, which has motivated the present researchers to look for fully automated schemes. This research article implements Analysis of Level Set based Novel Generic Model for Crosshatched Texture Segmentation

3.1 Dataset Description

This research article evaluates the performance of the proposed multi-resolution feature embedded level set model on the Brodatz texture dataset. In text classification, the Brodatz texture dataset, recorded from the University of Southern

California, is one of the popular datasets. The original dataset has rotated images generated using simple computer graphics methods. The statistical contribution of the Brodatz texture dataset is denoted in Table 1.

Table 1: Statistical contribution of the Brodatz texture dataset

Features	Values
Size	1.02 GB
Image format	8-bit gray-scale images
Texture patch size	640×640 pixels
Total number of samples	4480
Number of classes with unique samples	40
Number of classes	112

The sample images from Brodatz texture dataset are indicated in following Fig. 1.

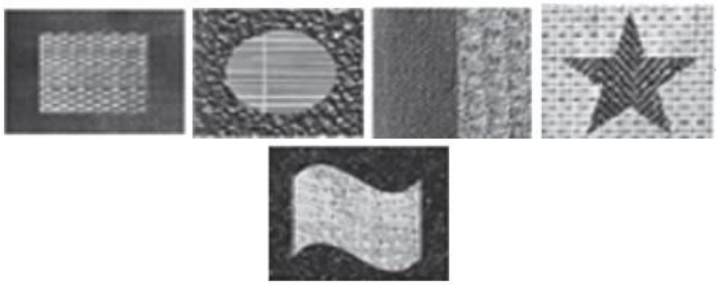

Fig.1: Brodatz texture dataset sample images (Source: MBT)

3.2 Pre-Processing

After acquiring the images from Brodatz texture dataset, the image pre-processing is carried out by using a histogram equalization technique that adjusts the crosshatch image intensities for improving the contrast of the images. Let 'f' be considered as the crosshatch image, which is denoted by a matrix integer pixel intensities 'm', that ranges between 0 to L-1. The histogram equalized crosshatch image g is mathematically determined in equation (1).

$$g_{i,j} = floor\,(L-1)\sum_{n=0}^{f(i,j)} p_n \quad (1)$$

Where, 'p' represents the normalized histogram value of crosshatch image 'f' with a bin-possible intensity, 'L' indicates the intensity value of range 256, and the term floor() rounds off the nearest integers, which are equivalent in transforming the pixel intensity value 'k', and it is mathematically denoted in following equation (2).

$$T(k) = floor(L-1)\sum_{n=0}^{k} p_n \quad (2)$$

The pixel intensities 'f' and 'g' are considered as the continuous random values of X=Y on [0, L-1] in the transformation section, which is mathematically defined in following equation (3).

$$Y = T(X) = (L-1)\int_0^x p_X(x)dx \quad (3)$$

Where 'T' indicates the cumulative distributive function of 'X' multiplied by L-1 and 'Px' represents the probability density function of crosshatch image 'f'. In addition to this, 'Y' is represented by $T(X)$, which is uniformly distributed on [0 ,L-1] namely $pY(y)=1/(L-1)$, and it is mathematically defined in following equations (4), (5), and (6).

$$\int_0^y p_Y(z)dz = \frac{1}{L-1} = \int_0^{T^{-1}(y)} p_X(w)dw \quad (4)$$

$$\frac{d}{dy}\left(\int_0^y p_Y(z)dz\right) = p_Y(y) = p_X(T^{-1}(y))\frac{d}{dy}(T^{-1}(y)) \quad (5)$$

$$\frac{dT}{dx}_{|x=T^{-1}(y)}\frac{d}{dy}(T^{-1}(y)) = (L-1)p_X(T^{-1}(y))\frac{d}{dy}(T^{-1}(y)) = 1 \quad (6)$$

where, $pY(y)=1/(L-1)$.

3.3 Level Set Model for Multi Resolution Based Crosshatched Texture Segmentation

In the proposed model, the pre-processed crosshatch image is constructed with two different crosshatched textures that have subjective boundaries. After pre-processing, the next step is selecting the correct size of the frequency domain filter, which is automated. The results obtained are integrated with a level set based active contour model that addresses the segmentation of crosshatched texture images. Any noise incurred during histogram equalization is eliminated by a post-processing step, using morphological processing.

4. Results and Discussion

This research article implements the proposed multi-resolution feature embedded level set model using a Matlab software environment. An extensive experimental analysis is performed on an Intel core i5-6200U computer processing unit, an 8 GB Random Access Memory, and a Linux operating system. The segmentation performance of the proposed multi-resolution feature embedded level set model is analyzed using an evaluation measure by the name of the IoU index. It is a statistical measure used for gauging the similarity and diversity of sample sets, where A and B indicate ground truth and segmented regions. It is mathematically stated in equation (7).

$$I(A,B) = \frac{|A \cap B|}{|A \cup B|} = \frac{|A \cap B|}{|A|+|B|-|A \cap B|} \quad (7)$$

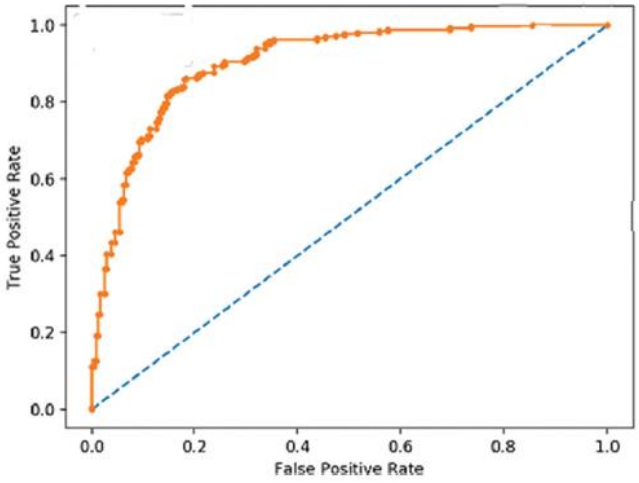

Fig. 4: ROC curve of the proposed model

On the other hand, the classification performance of the proposed multi-resolution feature embedded level set model is validated using evaluation measures like accuracy, recall, precision and f1-score, which are stated in equations (8), (9), (10) and (11). True Positive is denoted as (TP), False Positive as (FP), True Negative as (TN), and False Negative as (FN). Meanwhile, the Receiver Operating Characteristic (ROC) curve of the proposed model is stated in Fig 4.

$$Accuracy = \frac{TP+TN}{TP+TN+FP+FN} \times 100 \quad (8)$$

$$Recall = \frac{TP}{TP+FN} \times 100 \quad (9)$$

$$Precision = \frac{TP}{TP+FP} \times 100 \quad (10)$$

$$F1-score = \frac{2 \times Precision \times Recall}{Precision+Recall} \times 100 \quad (11)$$

4.1 Quantitative Evaluation in Terms of Segmentation

The proposed multi-resolution feature embedded level set model is tested, and the results obtained are verified in terms of the IoU index. The segmentation results of the proposed multi-resolution feature embedded level set model are mentioned in Table 2 and Fig. 5.

The original images with two crosshatched textures are acquired from the Brodatz texture dataset, and their subjective boundaries are represented in Fig. 5(a). The histogram results of the original image are shown in Fig. 5(b), and the automated filter size selection of the developed algorithm is shown in Fig. 5(c). The segmentation results of the level set algorithm are shown in Fig. 5(d). Any noise encountered during the histogram process is eliminated by opening and closing the morphological image processing, as shown in Fig. 5(e). The filter size selection is vital to performing proper segmentation in the original texture image. The algorithm initiates with a 3×3 filter size and then increases the filter size until the filter size equals the mean of the image partition. If the above condition is satisfied, the value of the lower cluster is used as the filter size.

The segmented results are validated by using the IoU index value, which is presented in Table 2, about IoU value is one. The IoU index of the image under study is greater than 0.9, which indicates that the proximity with the initial image is excellent, as shown in Table 2. The experimental outcome indicates that the proposed model can segment the region of interest in close correspondence with the texture image. The proposed multi-resolution feature embedded level set model is compared with MixNCut. The proposed segmentation model achieves precise accuracy on all the crosshatched texture images. It is measured using “raw” pixels that identify optimum segmentation. The proposed segmentation model significantly outperforms the existing segmentation model MixNcut. The

experimental results of the proposed and the existing segmentation models, in terms of running time and IoU index, are shown in Table 2.

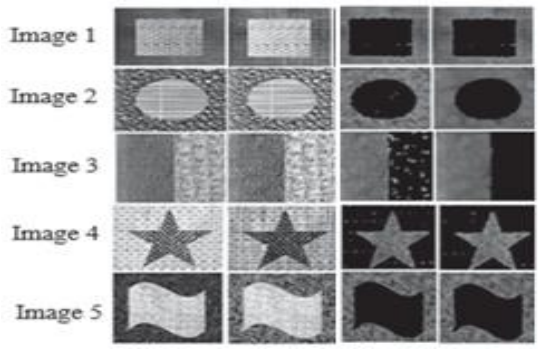

Fig. 5: Segmented output image (a) original image (Crosshatched) constructed from Brodatz texture dataset, b) histogram pre-processed image, (c) Segmented image through level set Algorithm, and (d) opening and closing results (Morphological Image Processing)

Table 2: Segmentation results in terms of IoU index value and running time

Index	Image 1		Image 2		Image 3		Image 4		Image 5	
Model	MixNcut [26]	Proposed	MixNcut [26]	Proposed	MixNcut [26]	Proposed	MixNcut [26]	Proposed	MixNcut [26]	Proposed
IoU	0.96	0.98	0.93	0.95	0.92	0.95	0.93	0.97	0.94	0.95
Time (sec)	9.09	6.30	6.61	5.42	7.15	5.35	8.05	5.72	7.89	5.81

4.2. Quantitative Evaluation in Terms of Classification

In the classification section, the proposed multi-resolution feature embedded level set model is tested with different classification techniques, namely: random forest, K-Nearest Neighbor (KNN), Support Vector Machine (SVM), and Multi-SVM (MSVM) using f1-score, accuracy, precision, and recall with different cross fold validations: 5 and 10 folds. By inspecting Tables 3 and 4, it is seen that the combination of multi-resolution feature embedded level set model with histogram equalization and MSVM has obtained higher classification performance in five-fold cross-validation with f1-score of 98.90%, accuracy of 99.82%, precision of 99.12%, and recall of 98.88% on the Brodatz texture dataset. The graphical depiction of the proposed multi-resolution feature embedded level set model with different classifiers and testing percentages is shown in Fig. 6 and 7.

As seen in the comparative analysis in Table 5, the proposed multi-resolution feature embedded level set model with MSVM achieved comparatively higher classification results when related to a model named modified CNN with WOA. The proposed model gained an f1-score of 98.90%, accuracy of 99.82%, precision of 99.12%, and recall of 98.88% on the Brodatz texture dataset. However, the modified CNN with WOA has obtained an accuracy of 99.71%, precision of 96.70%, recall of 95.80%, and f1-score of 96.20% on the Brodatz texture dataset. As depicted in the literature survey section, the proposed model effectively resolves the problems of higher computational time and achieves better segmentation and classification performance.

Table 3: Experimental results of the proposed model with five-fold cross-validation (80:20% training and testing)

Classifiers	Without histogram equalization				With histogram equalization			
	F1-score (%)	Accuracy (%)	Precision (%)	Recall (%)	F1-score (%)	Accuracy (%)	Precision (%)	Recall (%)
Random forest	90.34	91.76	93.23	89.28	93.24	95.30	96.66	92.20
KNN	92.95	92.56	92.45	93.33	95.90	98.24	96.32	97
SVM	93.73	92.34	92.37	92.28	97.74	99.22	98.32	97.22
MSVM	94.34	93.43	92.10	92.90	98.90	99.82	99.12	98.88

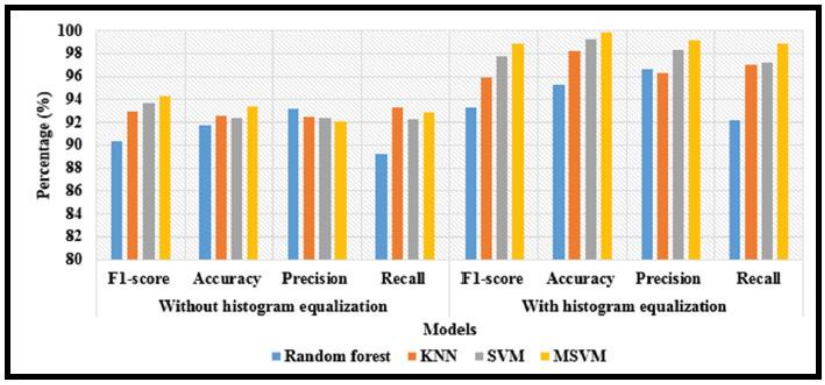

Fig.6: Graphical depiction of the proposed model with five-fold cross-validation (80:20% training and testing)

Table 4: Experimental results of the proposed model with ten-fold cross-validation (90:10% training and testing)

Classifiers	Without histogram equalization				With histogram equalization			
	F1-score (%)	Accuracy (%)	Precision (%)	Recall (%)	F1-score (%)	Accuracy (%)	Precision (%)	Recall (%)
Random forest	88.12	90.43	91.13	84.24	92.20	94.38	93.62	90.28
KNN	90.44	90.55	91.15	90.34	92.90	94.28	93.34	94.07
SVM	92.66	91.55	90.36	87.99	93.79	95.20	95.35	94.25
MSVM	92.38	91.49	90.18	88.95	94.98	95.83	95.17	94.87

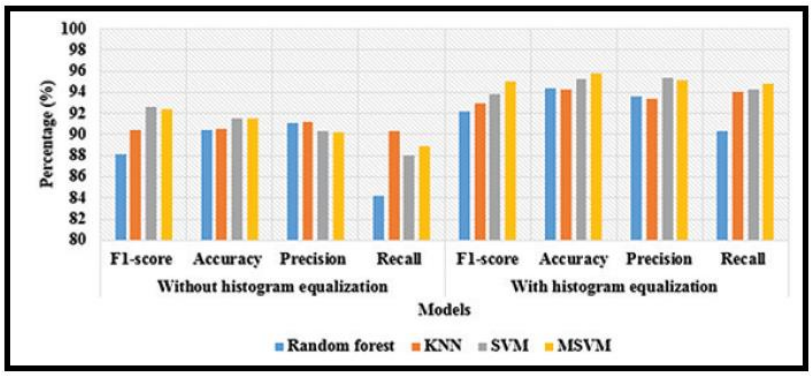

Fig.7: Graphical depiction of the proposed model with ten-fold cross-validation (90:10% training and testing)

Table 5: Comparative results between the proposed and the existing models

Models	F1-score (%)	Accuracy (%)	Precision (%)	Recall (%)
Modified CNN with WOA [20]	96.20	99.71	96.70	95.80
Multi-resolution feature embedded level set with MSVM	98.90	99.82	99.12	98.88

5. Conclusion

As discussed in this paper, a variational model, which is efficient for cross-hatched texture analysis, has been demonstrated. In image processing applications, image segmentation and shape detection are the main pre-processing steps for object detection. This paper proposes an effective model for computing the appropriate features and the filter size selection in unsupervised texture segmentation. For any texture analysis, it is important to select and identify filter size. Hence, the proposed model determines the minimum size of the filter for texture feature extraction to enhance discrimination and segmentation capabilities. This study introduces a multi-resolution feature embedded level set model, which segments challenging images like cross-hatched texture images acquired from the Brodatz texture dataset. The experimental results show that the proposed model provides longer-range interactions and captures the complex region appearances. The proposed segmentation model with MSVM classifier has achieved a classification accuracy of 99.82%, which is superior to other models. The proposed model is practical and robust and is

employed for other dissimilar types of texture images in future work. The proposed research is a generic solution for chemical studies, drug discoveries, precision agriculture, industrial equipment quality control, and medical equipment analysis.

REFERENCES

1. Ireri, D., Belal, E., Okinda, C., Makange, N., & Ji, C. (2019). A computer vision system for defect discrimination and grading in tomatoes using machine learning and image processing. Artificial Intelligence in Agriculture, Elsevier, 2, 28-37.
2. Devaraj, A., Rathan, K., Jaahnavi, S., & Indira, K. (2019, April). Identification of plant disease using image processing technique. In 2019 International Conference on Communication and Signal Processing (ICCSP) (pp. 0749-0753). IEEE.
3. Hoang, N. D., & Tran, V. D. (2019). Image processing-based detection of pipe corrosion using texture analysis and metaheuristic-optimized machine learning approach. Computational intelligence and neuroscience, 2019.
4. Shakeri-Zadeh, A. (2019). How can molecular micro-CT imaging revolutionize drug discovery?. Expert Opinion on Drug Discovery, 14(9), 849-853.
5. Sharifi, M., Attar, F., Saboury, A. A., Akhtari, K., Hooshmand, N., Hasan, A., ... & Falahati, M. (2019). Plasmonic gold nanoparticles: Optical manipulation, imaging, drug delivery and therapy. Journal of Controlled Release, Elsevier, 311, 170-189.
6. Cordeiro, L. S., Lima, J. S., Ribeiro, A. I. R., Bezerra, F. N., Rebouças Filho, P. P., & Neto, A. R. R. (2019, October). Pill image classification using machine learning. In 2019 8th Brazilian Conference on Intelligent Systems (BRACIS) (pp. 556-561). IEEE.
7. Fan, L., Zhang, F., Fan, H., & Zhang, C. (2019). Brief review of image denoising techniques. Visual Computing for Industry, Biomedicine, and Art, 2, 1-12.
8. Chen, X., Qi, W., & Xi, L. (2019). Deep-learning-based motion-correction algorithm in optical resolution photoacoustic microscopy. Visual Computing for Industry, Biomedicine, and Art, Springer, 2, 1-6.
9. Segura, Á., Diez, H. V., Barandiaran, I., Arbelaiz, A., Álvarez, H., Simões, B., ... & Ugarte, R. (2020). Visual computing technologies to support the Operator 4.0. Computers & Industrial Engineering, 139, 105550.
10. Parekh, P., Patel, S., Patel, N., & Shah, M. (2020). Systematic review and meta-analysis of augmented reality in medicine, retail, and games. Visual computing for industry, biomedicine, and art, Springer, 3, 1-20.
11. Kociołek, M., Strzelecki, M., & Obuchowicz, R. (2020). Does image normalization and intensity resolution impact texture classification?. Computerized Medical Imaging and Graphics, Elsevier, 81, 101716.
12. Elahi, GM Mashrur E., Sanjay Kalra, Lorne Zinman, Angela Genge, Lawrence Korngut, and Yee-Hong Yang. "Texture classification of MR images of the brain in ALS using M-CoHOG: A multi-center study." Computerized Medical Imaging and Graphics, Elsevier, 79 (2020): 101659.
13. Simon, P., & Uma, V. (2020). Deep learning based feature extraction for texture classification. Procedia Computer Science, Elsevier, 171, 1680-1687.
14. Barman, U., & Choudhury, R. D. (2020). Soil texture classification using multi class support vector machine. Information processing in agriculture, 7(2), 318-332.
15. Xu, X., Li, Y., & Wu, Q. J. (2021). A compact multi-pattern encoding descriptor for texture classification. Digital Signal Processing, Elsevier, 114, 103081.
16. Condori, R. H., & Bruno, O. M. (2021). Analysis of activation maps through global pooling measurements for texture classification. Information Sciences, 555, 260-279.
17. Kashyap, V., & Ramkumar, P. (2021). Comprehensive analysis of geometrical parameters of crosshatched texture for enhanced tribological performance under biological environment. Proceedings of the Institution of Mechanical Engineers, Part J: Journal of Engineering Tribology, 235(2), 434-452.
18. Hashim, N., & Hamid, J. R. A. (2021, May). Multi-Level Image Segmentation for Urban Land-Cover Classifications. In IOP Conference Series: Earth and Environmental Science (Vol. 767, No. 1, p. 012024). IOP Publishing.
19. Dagdelenler, G., Ercanoglu, M., & Sonmez, H. (2021). Semi-automatic Landslide Inventory Mapping with Multiresolution Segmentation Process: A Case Study from Ulus District (Bartin, NW Turkey). Understanding and Reducing Landslide Disaster Risk: Volume 2 From Mapping to Hazard and Risk Zonation 5th, Springer, 87-93.

20. Mikeš, S., & Haindl, M. (2021). Texture segmentation benchmark. IEEE Transactions on Pattern Analysis and Machine Intelligence, 44(9), 5647-5663.
21. Liu, Y., Zhang, Z., Liu, X., Wang, L., & Xia, X. (2021). Efficient image segmentation based on deep learning for mineral image classification. Advanced Powder Technology, Elsevier, 32(10), 3885-3903.
22. Kumari, N., Kr. Bhatt, A., Kr. Dwivedi, R., & Belwal, R. (2021). Hybridized approach of image segmentation in classification of fruit mango using BPNN and discriminant analyzer. Multimedia Tools and Applications, 80, 4943-4973.
23. Rezaei, Z. (2021). A review on image-based approaches for breast cancer detection, segmentation, and classification. Expert Systems with Applications, Elsevier, 182, 115204.
24. Moghadas-Dastjerdi, H., Sannachi, L., Wright, F. C., Gandhi, S., Trudeau, M. E., Sadeghi-Naini, A., & Czarnota, G. J. (2021). Prediction of chemotherapy response in breast cancer patients at pre-treatment using second derivative texture of CT images and machine learning. Translational Oncology, 14(10), 101183.
25. Möller, J., Bartsch, A., Lenz, M., Tischoff, I., Krug, R., Welp, H., ... & Miller, D. (2021). Applying machine learning to optical coherence tomography images for automated tissue classification in brain metastases. International Journal of Computer Assisted Radiology and Surgery, Springer, 16, 1517-1526.
26. Tharsanee, R. M., Soundariya, R. S., Kumar, A. S., Karthiga, M., & Sountharrajan, S. (2021). Deep convolutional neural network–based image classification for COVID-19 diagnosis. In Data Science for COVID-19 (pp. 117-145). Academic Press.
27. Okwuashi, O., Ndehedehe, C. E., Olayinka, D. N., Eyoh, A., & Attai, H. (2021). Deep support vector machine for PolSAR image classification. International Journal of Remote Sensing, 42(17), 6498-6536.
28. Jha, R. K., & Swami, P. D. (2021). Fault diagnosis and severity analysis of rolling bearings using vibration image texture enhancement and multiclass support vector machines. Applied Acoustics, 182, 108243.
29. Jusman, Y., Anam, M. K., Puspita, S., Saleh, E., Kanafiah, S. N. A. M., & Tamarena, R. I. (2021, September). Comparison of dental caries level images classification performance using knn and svm methods. In 2021 IEEE International Conference on Signal and Image Processing Applications (ICSIPA) (pp. 167-172). IEEE.